

Aeromagnetic Data Interpretation and Source Body Evaluation using Standard Euler Deconvolution Technique in Obudu area, Southeastern Nigeria

C. C. Agoha¹, C. N. Onwubuariri², T. I. Mgbejedo^{3*}, U. C. Amasike¹, C. B. Agbakwuru⁴, J. O. Njoku¹, C. C. Z. Akaolisa¹, I. A. Omenikolo⁴, I. J. Ofoh¹

¹ Department of Geology, Federal University of Technology, P.M.B. 1526, Owerri, Imo State, Nigeria

² Department of Physics, Michael Okpara University of Agriculture, P.M.B. 7267, Umudike, Abia State, Nigeria

³ Geophysical Section, Arab Center for Engineering Studies, Doha, Qatar

⁴ Department of Physics/Electronics, Federal Polytechnic Nekede, P.M.B. 1036, Owerri, Imo State, Nigeria

Received June 7, 2023; Accepted September 14, 2023

Abstract

In order to interpret the airborne magnetic data and to evaluate the approximate location, depth, and geometry of the magnetic sources within Obudu area using standard Euler deconvolution method, high resolution aeromagnetic data over the area was processed digitally and analyzed using Oasis Montaj 8.5 software. Data analysis and enhancement techniques including reduction to equator, horizontal derivative, first and second vertical derivatives, upward continuation and regional-residual separation were carried out. Standard Euler deconvolution for structural indices of 0, 1, 2, and 3 were obtained. Results show that the total magnetic intensity ranges from -122.9nT to 147.0nT, regional intensity varies between -106.9nT to 137.0nT, while residual intensity ranges between -51.5nT to 44.9nT indicating the masking effect of deep-seated structures over surface and shallow subsurface materials. Results also show that the positive residual anomalies have a NE-SW orientation which coincides with the trend of major geologic structures in the area. Euler deconvolution for all the structural indices has depth to magnetic sources ranging from <0m to >2000m. Interpretation of the various structural indices revealed the locations and depths of the source bodies and the existence of geologic models including sills, dykes, pipes, and spherical structures. This area is characterized by shallow basement materials and represents a good prospect for solid mineral exploration.

Keywords: Magnetic sources; Obudu; Euler Deconvolution; Aeromagnetic data; Horizontal derivatives; Structural indices.

1. Introduction

The aim of magnetic geophysical surveying is to carry out an investigation of the subsurface geology of an area based on the anomalies observed in the Earth's magnetic field as a direct result of the magnetic properties of the underlying rocks [1]. Magnetic surveys can be performed in the air, on land, and at sea. It is widely applied and the operation speed of the aeromagnetic surveys makes this method a very attractive tool in the search for deposits of ore containing magnetic mineral [1]. It is a potential field technique and, in most cases, used to validate that an area is underlain by shallow seated basement rocks [2]. This method has a wide range of applications ranging from small-scale archaeological and engineering surveys to large-scale surveys done to evaluate geological structure on a regional basis [1].

One of the several methods employed in the determination of basement depth and depth to magnetic source bodies in an area is the standard Euler deconvolution technique. It is a technique employed in the determination of the approximate depth of subsurface magnetic sources. It is also applicable to any other magnetic data of homogeneous field [3]. This technique is an interpretation method that is semi-automatic and it is regularly applied with gravity and magnetic datasets. In this technique, a given type of magnetic source is specified by the

term known as structural index, and the approximate location of this source is also provided. This technique is relatively simple to implement and use, hence, it is a tool for fast initial interpretation. Euler deconvolution maps reveal good constraints on the horizontal position of an anomaly source. According to [4], accuracy of the results of Euler deconvolution can be significantly improved by calculating the solution space of individual data points and picking common source locations.

Several authors including [5-7], and others have studied the basement depths and depth to magnetic sources of various areas using Euler deconvolution method. These previous authors made telling contributions to the subject of Euler deconvolution in their various locations of study. Several of these authors, however, did not analyze all the structural indices from 0 to 3 which in most cases respectively reveal varying geologic models. This study has also been made with a much-improved software package which revealed more detailed source body information about the study area.

This study is therefore, aimed at interpreting the airborne magnetic data and determining the approximate location, depth, and geometry of magnetic source bodies within Obudu area, Southeastern Nigeria.

2. Location and geology of the study area

Obudu area is located in Cross River State of Southeastern Nigeria. This area lies within latitudes $6^{\circ}30'N$ to $7^{\circ}00'N$ and longitudes $9^{\circ}00'E$ to $9^{\circ}30'E$. The study area shares boundaries with Obanliku to the east, Bekwarra and Ogoja to the west, Boki to the south, and Benue State to the north. Figure 1 shows the map of Cross River State showing the study area.

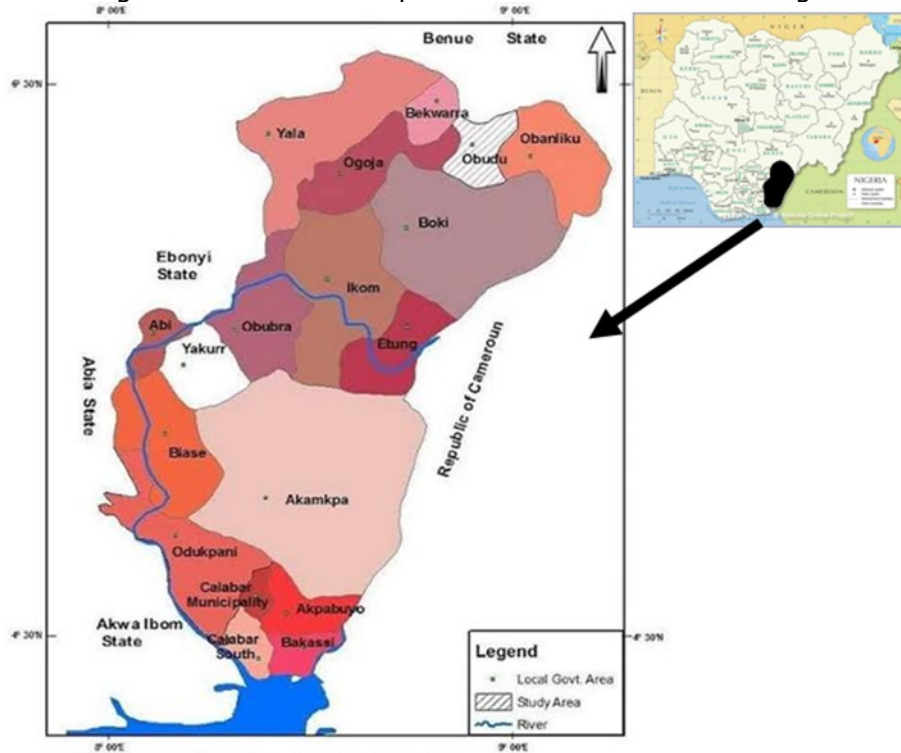


Figure 1. Map of Cross River State, Nigeria showing Obudu area (Source: Cartography/GIS unit, Department of Geography and Environmental Sciences, University of Calabar).

Geologically, there is an outcrop of the Nigerian precambrian basement in Obudu area. This area is underlain dominantly by gneissose rocks having migmatitic characteristics [9]. The hornblende-granite gneiss is widespread in Obudu area, in fact, gneissose rocks cover about two-thirds of the entire area [9]. There is a banding arrangement of the gneisses with quartz and plagioclase being the major minerals in the leucosome. Hornblende and biotite are found

in the paleosome. According to [9], the gneissose rocks clearly show bands having alterations of dark and light colour. The rocks are also described as being mesocratic and medium grained. In addition to the hornblende granite gneiss and granite gneiss, other rock types in this area include migmatite, porphyritic granite, charnockite, Asu River Group, and Eze Aku Formation. Figure 2 shows the geological map of the study area.

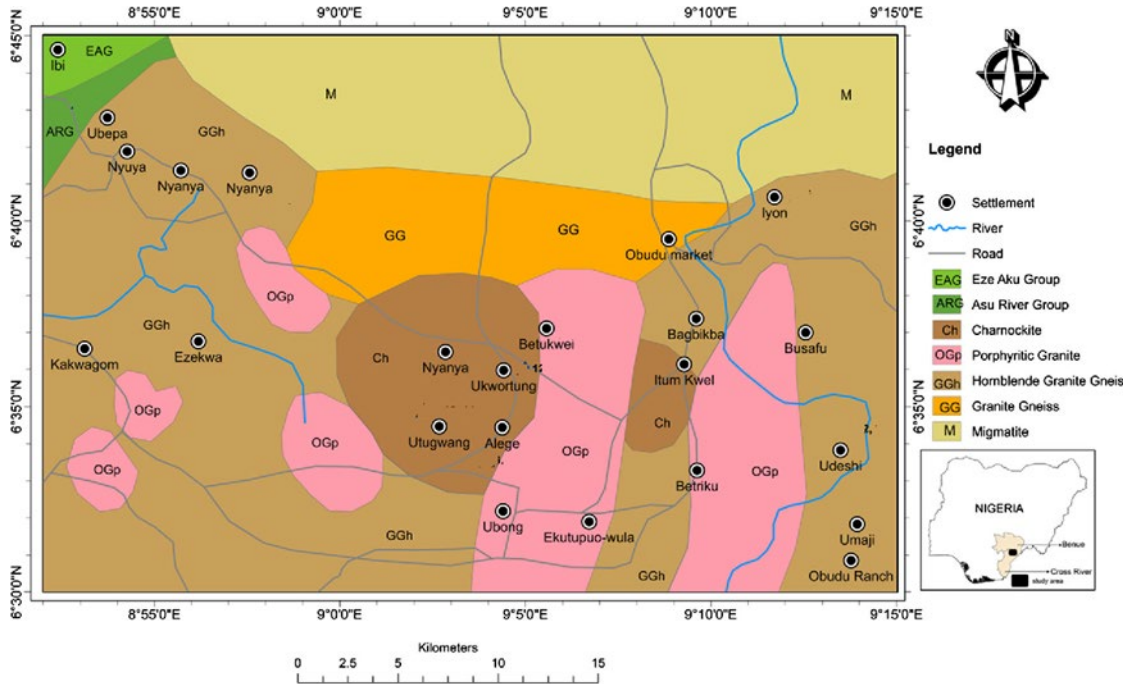


Figure 2. Geological map of Obudu area (after [10]).

3. Methodology

3.1. Materials

The high resolution aeromagnetic data used for this study was obtained from the Nigerian Geological Survey Agency (NGSA). This data was acquired between 2005 and 2009 and is part of the newly acquired digital aeromagnetic data for most parts of Nigeria. The data was acquired at a line spacing of 500m and a terrain clearance of 80m and the flight direction was along the northwest-southeast (NW-SE). Fugro Airborne surveys carried out this acquisition. A portion of the nationwide aeromagnetic grid covering Obudu area with latitude and longitude as stated in the location section of this paper was made available for this study by NGSA. The 2005 International Geomagnetic Reference Field (IGRF) formula was used to remove the geomagnetic gradient from this data. The resolution of this data is very high when compared with the data previously acquired and used for interpretation in this area. The Geosoft Oasis Montaj software, version 8.5 was used for data analysis and enhancement.

3.2. Methods

Initial processing of this data which includes editing and filtering was carried out by contractors named Paterson Grant and Watson Ltd. They performed cultural editing which takes care of rough effects as a result of interference due to local structures in the area. Corrections for diurnal variations were done through subtraction of filtered and IGRF corrected ground station data. Upon IGRF and diurnal corrections, data variations occurring at traverse and tie line recordings intersections were taken care of through a leveling process. There was interpolation of the products into a regular grid which then gave rise to the total magnetic intensity (TMI) map.

Reduction to equator (RTE) was then applied to the TMI data. This is a process of transformation of the TMI field at its declination and inclination observed to that of the magnetic equator. This is usually done to solve problems that occur due to magnetic data having low latitude. Reduction to equator is expressed mathematically in Eqn. 1 [3] as

$$RTE = \sin I + i \cos I \sin (D - \theta)^2 \quad (1)$$

where I = geomagnetic inclination; D = geomagnetic declination; $\sin I$ = amplitude component; $i \cos I \sin (D - \theta)^2$ = phase component.

This was followed by data enhancement of the raw total magnetic intensity map in order to greatly enhance anomalies of interest. Fast Fourier Transform (FFT) was used to carry out this enhancement in the spatial frequency domain where the raw TMI was subjected to some filters. Horizontal derivative, first and second vertical derivatives, and upward continuation are some of the enhancement processes carried out in this study. More detail on these enhancement processes can be found in [11-14]. Standard Euler deconvolution for structural indices of 0, 1, 2, and 3 was also carried. Residual magnetic intensity map was obtained by subtracting the regional magnetic intensity from the total magnetic intensity using the polynomial fitting method.

As described earlier in introduction section, the standard Euler deconvolution is a very important technique that enables the determination of the location as well as the depth and geometry of magnetic sources in a given area. The Euler homogeneity equation [13] is a formula relating the components of the total magnetic field to the source location with the degree of homogeneity which can be said to be the structural index. This relationship is expressed in Eqn. 2 as

$$(x-x_0) \partial T/\partial x + (y-y_0) \partial T/\partial y + (z-z_0) \partial T/\partial z = N(B-T) \quad (2)$$

where T = total magnetic field measured at x , y and z ; x_0 , y_0 and z_0 = position of the magnetic body; N = degree of homogeneity interpreted as the structural index; B = background value of the total magnetic intensity.

The standard Euler deconvolution technique is based on this equation. The technique produces estimates of depth while leveraging on a structural index. A combination of depth estimates and structural index is more than capable of identifying and computing estimates of depth for a range of geologic models like sills, dykes, pipes, horizontal cylinders, spherical structures and geologic contacts. It is important to note that each geologic model has a structural index peculiar to it. According to [15], spherical structures are characterized by a magnetic structural index of 3, pipes and horizontal cylinders are characterized by structural index of 2, dykes and sills by structural index of 1, thick steps by structural index of 0.5 while geologic contacts are characterized by structural index of 0. The workflow employed in data analysis and enhancement is shown in (Figure 3) while (Figure 4) shows the workflow used for standard Euler deconvolution.

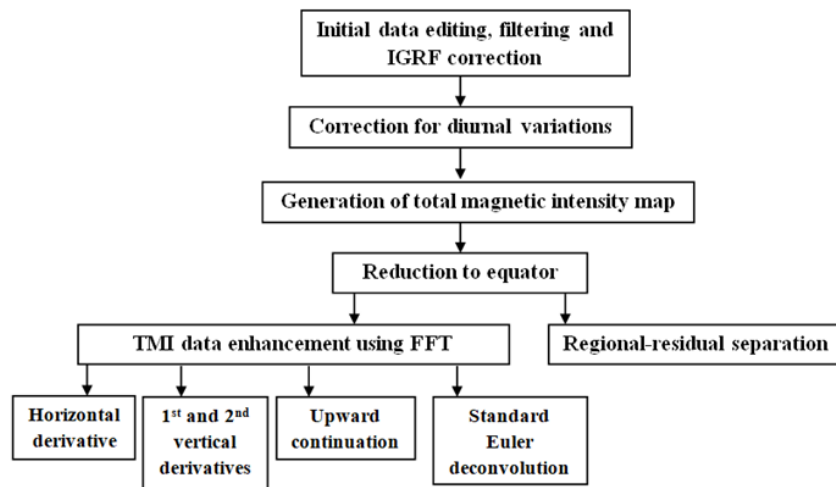


Figure 3. Workflow employed in data analysis and enhancement.

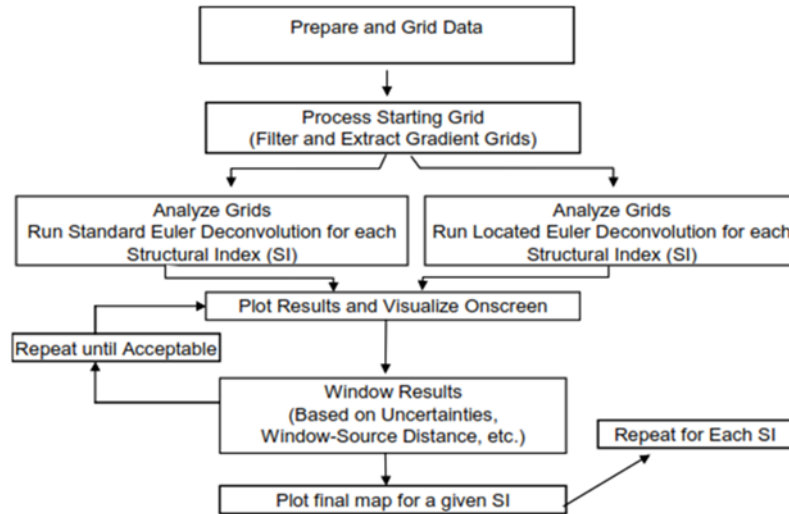


Figure 4. Workflow used for standard Euler deconvolution.

4. Results and discussion

4.1. Total magnetic intensity of the area

The total magnetic intensity anomaly in this area ranges between -122.9nT to 147.0nT . About 70% of the entire area is characterized by positive anomaly while the remaining portions are of negative. High positive anomaly is observed in the northwestern axis with amplitude values reaching 147nT and a wavelength of about 31.4km . A similar high amplitude anomaly also exists in the southwest axis but with a shorter wavelength of about 27.7km . Bipolar anomalies exist between the northwest and southwest axes and the area separating them. A negative pole exists in this intervening area with amplitude of -122.9nT and wavelength of about 37km . Also, it is observed that a weak gradient limits the positive anomalies of the northwest and southwest from the area separating them. This is traceable to the overlapping intensity of the geological formations. Positive anomalies in the central and southern parts of the study area are limited by a high gradient and this can be linked to the presence of normal fault or fracture. The central and southern parts are characterized by heterogeneous magnetic anomalies and this is attributable to the magnetic susceptibilities of the heterogeneous basement materials in these areas. Figure 5 shows the total magnetic intensity map of the area.

4.2. Residual magnetic intensity of the area

Map of the residual magnetic intensity of the study area is shown in (Figure 6). Residual intensity anomaly in this area vary between -51.5nT and 44.9nT . Comparison of this map with the total intensity map shows a decrease in positive anomaly amplitude of 102.1nT and this clearly points to the fact that the effects of underlying materials mask the effects of surface and shallow subsurface materials. There is a marked disappearance of the magnetic highs observed in the northwestern (NW) and southwestern (SW) axes of the TMI map. On the other hand, areas of magnetic highs and lows observed on the TMI map are retained on the regional magnetic intensity map as shown in (Figure 7).

The positive residual anomalies are purely due to localized materials and tend to have a northeast-southwest (NE-SW) direction as also observed on the TMI map. This trend of positive residual anomalies is related to the directions of major geologic structures rich in magnetic minerals and will make it possible to locate them. According to [9], the direction of dominant foliation in the study area is N-S to NE-SW with 55° as the mean dip, hence, direction of magnetic anomalies is closely related with lines of tectonism. The magnetic peaks are broken and appear dissociated at close observation; these peaks are possibly as a result of intrusions in the area.

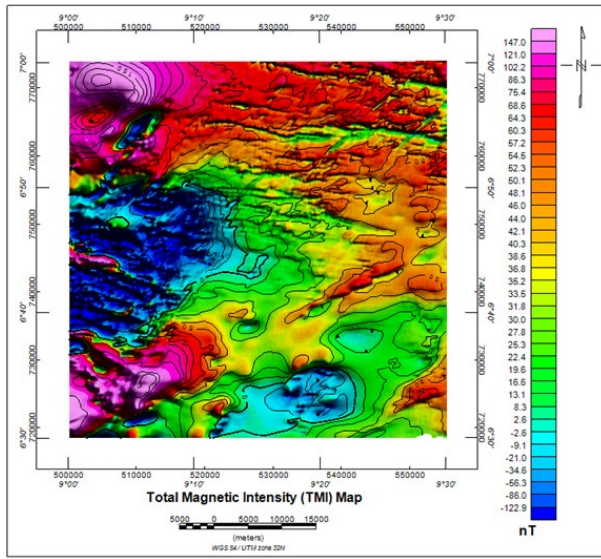


Figure 5. Total magnetic intensity map of the study area.

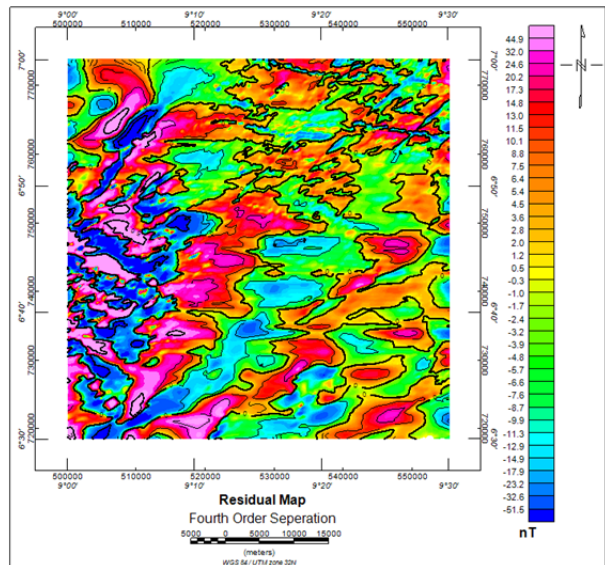


Figure 6. Fourth degree residual magnetic intensity map of the study area.

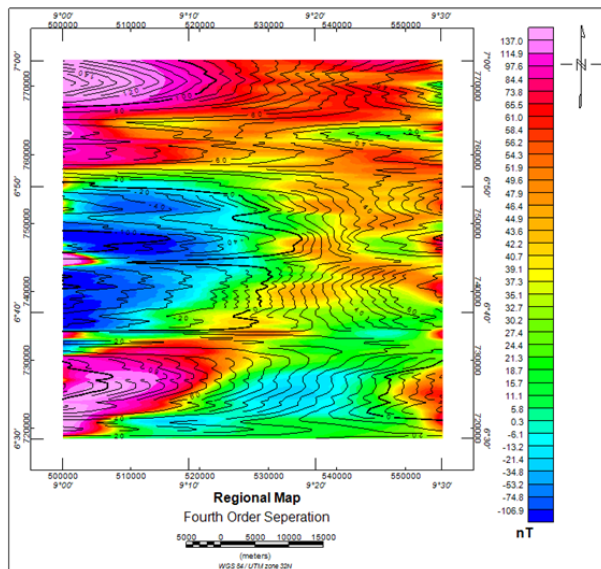


Figure 7. Fourth degree regional magnetic intensity map of the study area.

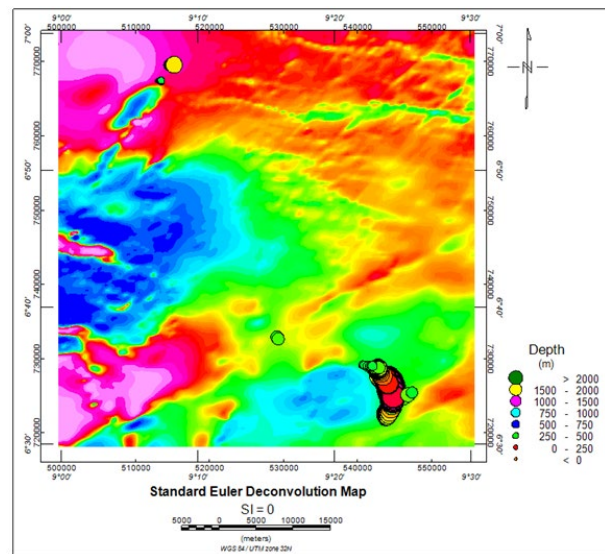


Figure 8. Standard Euler deconvolution map for structural index of 0.

The regional magnetic anomaly in this area range between -106.9nT and 137.0nT, showing a decrease in positive anomaly amplitude of 10nT. The decrease observed in residual anomaly is very much higher than that observed in regional anomaly and points to the fact that regional fields dominate the total fields in a given area. The regional field preserves most of the features of the total field as observed in the maps.

4.3. Standard Euler deconvolution

As described earlier, this is one of the techniques applied in the determination of depth and geometry of magnetic sources in an area. In the present study, Euler deconvolution for structural indices of 0, 1, 2 and 3 were carried out, each index revealing characteristic geologic model(s). Results of this process are superimposed on the upward continuation map of the

total magnetic intensity. Four maps as presented in (Figures 8, 9, 10 and 11) show results of the Euler technique for the four considered structural indices respectively. On each of the maps, the source bodies are represented by circular features of varying colours. Green represents deep-lying structural features sitting at a depth of more than 2000m while brown represents surface features lying less than 0m on the surface.

The map for structural index of 0 reveals the existence of mostly deep-seated and shallow-lying geologic contacts in this area. The deep-seated contacts lie above 1500m while the shallow ones lie about 250m and less. Clearly, these solutions are clustered in the southeastern part of the area.

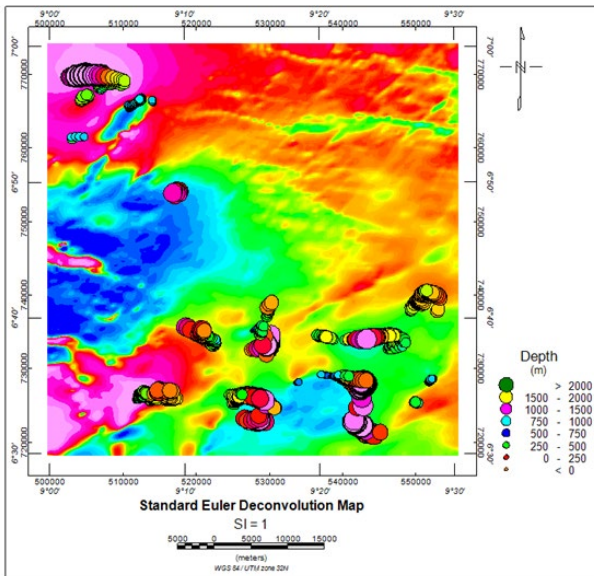


Figure 9. Standard Euler deconvolution map for structural index of 1.

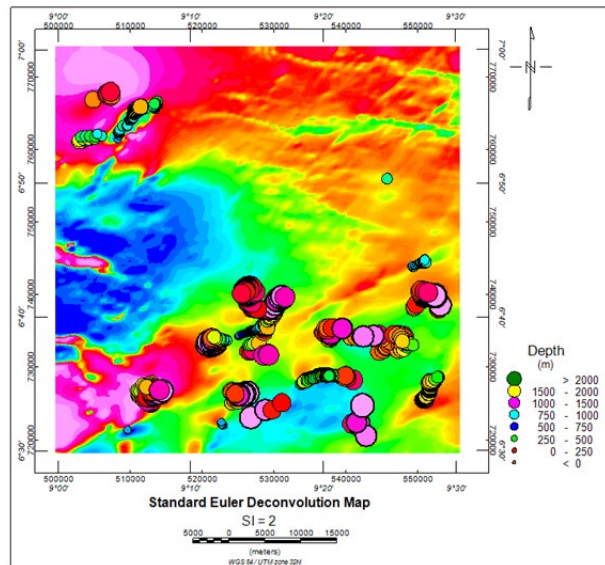


Figure 10. Standard Euler deconvolution map for structural index of 2.

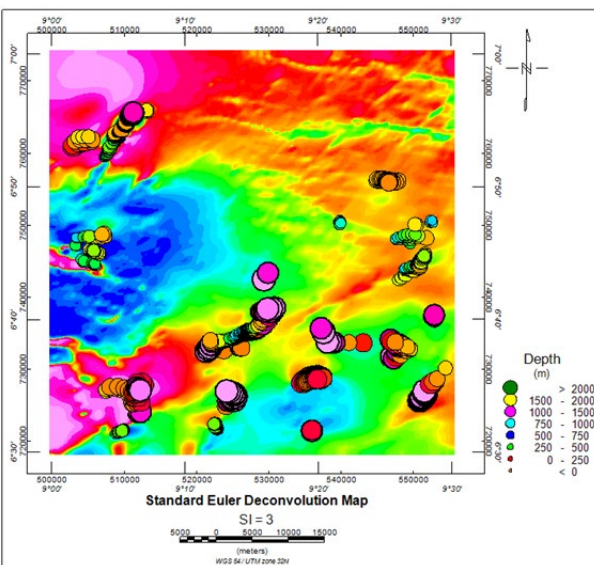


Figure 11. Standard Euler deconvolution map for structural index of 3.

The pattern of the clusters for structural index of 2 is very similar to those of structural index of 1 where most are in the south of the study area. This structural index is characteristic of magnetic sources having the geometry of pipes and horizontal cylinders. Most of these structures are sitting deep at depths of 1000m and above. There are also shallow-lying structures sitting at 250m and less. One remarkable occurrence in the maps for structural index of 1 and 2 is that across the entire northern axis of the study area, these cluster groups appear only in the northwestern axis. For these two structural indices (1 and 2), these cluster groups in the southern axis occur within an area of about 1,283.4 km².

Structural index of 3 reveals the existence of magnetic sources exhibiting spherical shapes. This implies that some of the magnetic sources in this area are spherically shaped and are clustered in various groups

mainly also in the south of the study area but more widespread than those of structural index of 1 and 2. Like in the structural indices earlier interpreted, most of these magnetic spheres are deep-seated, lying at depths of about 1000m and above. Some of these spheres lie between 500m to 1000m while the shallow ones lie less than 250m from the surface.

Most of the clustered solutions are limited in the southern axis implying that the sills, dykes, horizontal cylinders, pipes, and spherical structures are more prevalent in the southern part of this study area. For structural index of 3, these cluster groups which are more widespread in this case occur within an area of about 2,628.8 km².

5. Conclusion

High resolution airborne magnetic data over Obudu area have been leveraged on to interpret the magnetic characteristics of this area. Also, the much reliable standard Euler deconvolution technique has been utilized in the evaluation of the approximate location, depth, and geometry of magnetic sources in the area. Tectonic lines associated with the Pan-African mobile belt in Central Africa control the trend of residual anomaly and by extension mineralization in this area. Intrusions may be present in this environment as inferred from the peaks on the residual magnetic anomaly map. Also, shallow, moderate and deep-seated geologic structures including geologic contacts, dykes, sills, pipes, horizontal cylinders, and spheres are dominant in this area though most are situated within 1,283.4km² south of Obudu. The findings of this study clearly indicate that this location is very good for solid mineral prospectivity.

Acknowledgement

The authors appreciate the support, in the area of airborne magnetic data, of the Nigerian Geological Survey Agency (NGSA).

Funding: *The authors received no special funding for this research.*

Data Availability Statement *The data that support the findings of this study are available on request from the corresponding author.*

Declarations

Conflict of interest: *The authors declare that there are no conflicts of interest.*

Ethical Statement: *The paper reflects the authors' research and analysis in a truthful and complete manner.*

References

- [1] Kearey P, Brooks M, and Hill I. An introduction to geophysical exploration 3rd edition Blackwell Science Limited. 2002.
- [2] Agoha CC, Adejuwon BB, Mgbeojedo TI, Onwubuariri CN, Akiang FB, Ibeneme SI, Okechukwu SI, Ofoh IJ, and Njoku JO. Natural radioactivity assessment and geophysical interpretation of parts of Igarra area, Southern Nigeria. *Environmental Monitoring and Assessment*, 2022; 194(6): 438. <https://doi.org/10.1007/s10661-022-10055-2>.
- [3] Yandjimain J, Ndougsa-Mbarga T, Meying A, Bi-Alou MB, Ngoumou PC, Assembe SP, Ngoh JD, and Owono-Amougou OUI. Combination of tilt-angle and Euler deconvolution approaches to determine structural features from aeromagnetic data modeling over Akonolinga-Loum area (Centre-East Cameroon). *International Journal of Geosciences*, 2017; 8: 925-947. <https://doi.10.4236/ijg.2017.87053>.
- [4] Cooper GRJ. Euler Deconvolution with improved accuracy and multiple different structural indices. *Journal of China University of Geosciences*, 2008; 19(1): 72-76. [https://doi.org/10.1016/s1002-0705\(08\)60026-6](https://doi.org/10.1016/s1002-0705(08)60026-6).
- [5] Lawal TO, Salawu NB, Orosun MM, Ekpumoh JI, and Nwankwo LI. Application of 3-D Euler deconvolution technique to aeromagnetic data of Ilorin and Osi, Northcentral Nigeria. *Zimbabwe Journal of Science & Technology*, 2016; 11: 66-75.
- [6] El Dawi MG, Tianyou L, Hui S, and Dapeng L. Depth estimation of 2-d magnetic anomalous sources by using Euler deconvolution method. *American Journal of Applied Sciences*, 2004; 1(3): 209-214.
- [7] Oha IA, Onuoha KM, Nwegbu AN, and Abba AU. Interpretation of high resolution aeromagnetic data over southern Benue Trough, southeastern Nigeria. *J. Earth Syst. Sci.*, 2016; 125(2): 369-385.

- [8] Omenikolo IA, Emberga TT, and Opara AI. Basement depth re-valuation of anomalous magnetic bodies in the lower and middle Benue trough using Euler deconvolution and spectral inversion techniques. *World Journal of Advanced Research and Reviews*, 2022; 14(02): 129-145. <https://doi.org/10.30574/wjarr.2022.14.2.0356>.
- [9] Agbi I, and Ekwueme BN. Preliminary review of the geology of the hornblende biotite gneisses of Obudu Plateau, Southeastern Nigeria. *Global Journal of Geological Sciences*, 2019; 17: 75-83.
- [10] Adamu CI, and Duru CC. Composition, geotechnical characteristics and the potential for industrial use of some clay bodies in Obudu and its environs, Southeastern Nigeria. *Geotechnical and Geological Engineering*, 2020; 38: 6909-6920. doi: 10.1007/s10706-020-01424-0.
- [11] Nabighian MN, Grauch VJS, Hansen RO, LaFehr TR, Li Y, Peirce JW, Philips JD, and Ruder ME. The historical development of the magnetic method in exploration. *Geophysics*, 2005; 70: 33-61.
- [12] Reeves CV. *Aeromagnetic surveys, principles, practice and interpretation*. Geosoft. 2005.
- [13] Thompson DT. EULDPH: A new technique for making computer-assisted depth estimates from magnetic data. *Geophysics*, 1982; 47(1): 31-37.
- [14] Roest WR, Verhoef, J, and Pilkington M. Magnetic interpretation using the 3D analytic signal. *Geophysics*, 1992; 57: 116-125.
- [15] Reid B, Allsop JM, Granser H, Millet AJ, and Somerton IW. Magnetic interpretation in three dimensions using Euler deconvolution. *Geophysics*, 1990; 55(1): 80-91.

*To whom correspondence should be addressed: T. I. Mgbejedo, Geophysical Section, Arab Center for Engineering Studies, Doha, Qatar; e-mail: toomgbejedo@gmail.com
ORCID: 0000-0003-0818-1427*